

Deconvolution of Scanning Transmission Electron Microscopy Images of Ionomers

BRIAN P. KIRKMEYER¹, RICHARD C. PUETTER², AMOS YAHIL², KAREN I. WINEY¹

¹Department of Materials Science and Engineering, University of Pennsylvania, 3231 Walnut Street, Philadelphia, Pennsylvania 19104

²Pixon LLC, 9295 Farnham Street, San Diego, California, 92123

Received 10 September 2002; revised 15 November 2002; accepted 16 November 2002

ABSTRACT: Previously, we studied a variety of ionomer morphologies with scanning transmission electron microscopy (STEM). Other groups have found that deconvoluting STEM images dramatically improve the overall image quality and the detection of sub-nanometer-scale features. In this study, STEM images of nanometer-scale ion-rich aggregates were deconvolved via the Pixon method with a simulated electron probe. The image models are considerably sharper with significantly decreased noise levels, thus making the size and shape of the ionic aggregates easier to distinguish relative to those in the raw STEM images. Raw and deconvoluted images of Zn-neutralized poly(styrene-*ran*-methacrylic acid) ionomers containing spherical ionic aggregates indicate that the electron density varies smoothly from the edge to the center of the aggregates. Deconvolution also clarifies the issue of aggregate overlap in the STEM images. Furthermore, line scans across deconvoluted STEM images suggest that the three-dimensional density distribution of these nanoaggregates compares favorably with a radially symmetric Gaussian distribution as opposed to a uniformly dense sphere. The overall result of this work is that deconvolution of STEM images provide ways in which to better investigate the morphologies of ionomers. © 2003 Wiley Periodicals, Inc. *J Polym Sci Part B: Polym Phys* 41: 319–326, 2003

Keywords: ionomer; morphology; electron microscopy; STEM; deconvolution

INTRODUCTION

We previously published bright field and high-angle annular dark field scanning transmission electron microscopy (BF- and HAADF-STEM) images of ethylene- and styrene-based ionomers neutralized with various cations.^{1–5} These images reveal a wide variety of morphologies for the different chemistries and neutralizing cations. For example, a poly(ethylene-*ran*-methacrylic acid) melt neutralized with Zn (Zn-EMAA) contains

randomly distributed solid spherical ionic aggregates with an average diameter of 2.1 nm,⁴ whereas a poly(styrene-*ran*-methacrylic acid) solution neutralized with Cs (Cs-SMAA) contains randomly distributed vesicular ionic aggregates with a diameter range from 5 to 45 nm and a shell thickness of ~3 nm.¹ The number density of the aggregates in the projected images range from ~20,000 aggregates/ μm^2 for Zn-EMAA to ~50 aggregates/ μm^2 for Cs-SMAA. In this article, we focus on the physics of image creation and the need to deconvolve the electron probe from the STEM images.

The STEM that we use is equipped with a field-emission electron gun (FEG) that approxi-

Correspondence to: K.I. Winey (E-mail: winey@lrsm.upenn.edu)

Journal of Polymer Science: Part B: Polymer Physics, Vol. 41, 319–326 (2003)
© 2003 Wiley Periodicals, Inc.

mates a point source for the electron beam. As the electron beam travels down the microscope column, it is aligned by a series of lenses and apertures to focus at the plane of the specimen. Rutherford-type interactions between the electron beam and the nuclei in the specimen result in the scattering of electrons to certain angles. The Rutherford cross section for this scattering is

$$\frac{d\sigma(\theta)}{d\Omega} = \frac{\lambda_R^4 Z^2}{64\pi^4 a_0^2 \left[\sin^2 \frac{\theta}{2} + \left(\frac{\theta_0}{2} \right)^2 \right]^2} \quad (1)$$

where λ_R is the relativistically corrected electron wavelength, Z is the atomic number of the scattering atom, a_0 is the Bohr radius of the scattering atom, θ is the scattering angle of the electron, and θ_0 is the screening parameter (because of the electron cloud).⁶ This equation demonstrates the approximate Z^2 dependence of scattering on the atomic number, which is the basis for STEM imaging the high- Z , cation-rich nanoaggregates in ionomers.

When a point source is imaged, it appears as an Airy disc because of the diffraction that occurs at the outermost collection angles of the lenses.⁶ A profile of the Airy disc is shown in Figure 1(a). If the maximum from one source lies over the minimum from another source, the intensity profile of overlapping Airy discs has a slight dip in the middle [Fig. 1(b)]. The eye can distinguish this overlapping as separate features. This is the minimum resolvable distance (r_{th}) (i.e., resolution) in the image, given by

$$r_{th} = 0.61 \frac{\lambda}{\beta} \quad (2)$$

where λ is the electron wavelength (set by the accelerating voltage), and β is the maximum semiangle of collection of the objective lens aperture.⁶ For our JEOL 2010F, $r_{th} = 0.34$ nm. Features separated by greater than this distance can be distinguished from one another in an image.

In addition to knowing the minimum resolvable distance in the microscope, we must also be concerned with the pixel size in an acquired image. STEM is a digital imaging technique in that images are generated and recorded electronically. For our microscope the image size varies from 64×51 pixels to 4096×3264 pixels. The physical size corresponding to each pixel decreases with increasing either the image size or the magnifica-

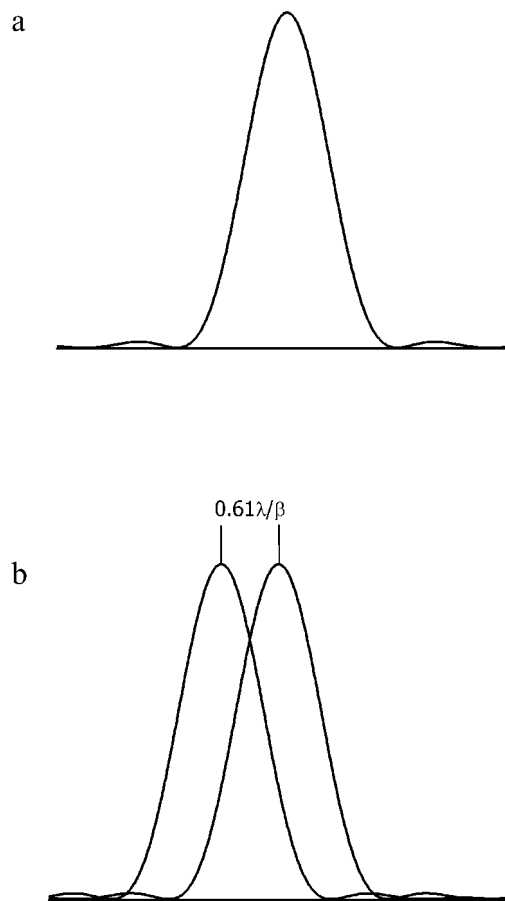


Figure 1. (a) Airy disc-scattering profile for a point source that arises from the diffraction that occurs at the outermost collection angles of the lenses. (b) Overlapping Airy disc-scattering profiles indicating the minimum resolvable distance (resolution) in an image.

tion at which the image is obtained. For a $500,000\times$ magnification image, the pixel size will decrease from 3.66 to 0.055 nm over our range of image sizes. Therefore, the accuracy and precision of our feature size measurements will increase when collecting larger image data files or at higher magnifications.

The specimen morphology is convolved with the microscope diffraction pattern to produce a STEM image. To obtain an accurate depiction of the specimen morphology, the image may need to be deconvolved of these microscopic contributions. Other groups have demonstrated the importance of deconvolving STEM images of sub-nanometer-scale morphologies. Kadavanich et al.⁷ used a maximum entropy method to reveal the crystal lattice of a CdSe nanocrystal that had previously been obscured by noise and microscopy physics. The morphologies of the ionomers are on the

nanometer-length scale, that is, an order of magnitude larger in size than the nanocrystal lattice. This study addresses the need to deconvolve STEM images of nanometer-scale morphologies in ionomers. A brief description of the deconvolution method is provided. Comparisons are made between images formed by the real probe in the microscope and those that are deconvolved with a simulated probe. In addition, two different aspects of the simulated probe are investigated—shape and size. Finally, and perhaps most interestingly, we begin to explore the structure within the ionic aggregates.

EXPERIMENTAL

Materials and Sample Preparation

Poly(styrene-*ran*-methacrylic acid) (SMAA) ionomers fully (100%) neutralized with Zn ($Z = 30$) were used in these experiments. The copolymer was bulk free-radical copolymerized from styrene and methacrylic acid monomers to an acid comonomer content of ~ 6 mol %. The copolymer was dissolved in a toluene/methanol (9/1 v/v) mixture and was neutralized with zinc acetate dihydrate in methanol. The neutralized ionomer was stirred overnight and then isolated via precipitation in ethanol and collected by siphoning off the supernatant. The powder was washed with ethanol, isolated again, and then dried under vacuum for 3 h at 150 °C.

Specimen Preparation

It was necessary to create specimens suitable for imaging in the microscope from the ionomer powders. The powders were compression-molded at 9000 N for 20 min at 150 °C. Material was iteratively added to the mold to facilitate the creation of fully dense sample discs. Visual inspection ensured that the discs were clear, that is, free of voids. Thin sections (100-nm nominal thickness) were microtomed from the discs at room temperature with a Reichert–Jung Ultracut S ultramicrotome with a diamond knife at a cutting speed of 0.4 mm/s. The sections were collected with a “wet” microtomy method in which sections were floated onto deionized water in the knife boat and collected on copper specimen grids. These grids were stored in a room temperature vacuum chamber until analysis in STEM. This specimen prepara-

tion technique has been demonstrated to preserve the bulk ionomer morphology.¹

STEM

Imaging was performed on a JEOL 2010F FEG STEM operated at 197 kV with a 0.7-nm probe size and a 50- μm condenser aperture. Images were collected with a Gatan BF scintillator detector and a JEOL high-angle annular dark field (HAADF) scintillator detector. For HAADF-STEM images, a detector collection angle range of 50–110 mrad was used. In BF mode, high-atomic-number species appear dark, whereas in the HAADF mode, high-atomic-number species appear bright in the image. We have demonstrated that BF and HAADF images provide the same information about ionic aggregates in ionomers.³ The image file size for these experiments was 1024×816 pixels. False coloring of the images and measuring of ionic aggregate dimensions were done with Adobe Photoshop 5.0. Zooming in on the images facilitated the measurements.

DECONVOLUTION METHOD

The Pixon method of image deconvolution uses a minimum-complexity model to separate data from noise. A complete description of the Pixon method, as well as descriptions of image reconstruction methods in general, is given elsewhere.⁸ The technique was originally applied to astronomical imaging data but has been applied to atomic-scale STEM imaging of crystals.⁹ Here we investigate whether deconvolution is important in the imaging of nanometer-scale morphologies, that is, one order of magnitude larger.

A minimum-complexity model has the twofold benefit of enabling an efficient image representation as well as an optimal manner of sorting out signal from noise. If the minimum number of parameters can adequately fit the data, then any additional parameters will fit the noise and any fewer parameters will insufficiently fit the data. This means that the data are not overinterpreted. Because the noise is being rejected, a weak real structure that meets statistical acceptance criteria is enhanced. The resulting deconvoluted image is noise free and contains only signal.

The Pixon deconvolution method takes a raw STEM image and removes image blur caused by the electron optics. Deblurring is performed by deconvolving the appropriate point response func-

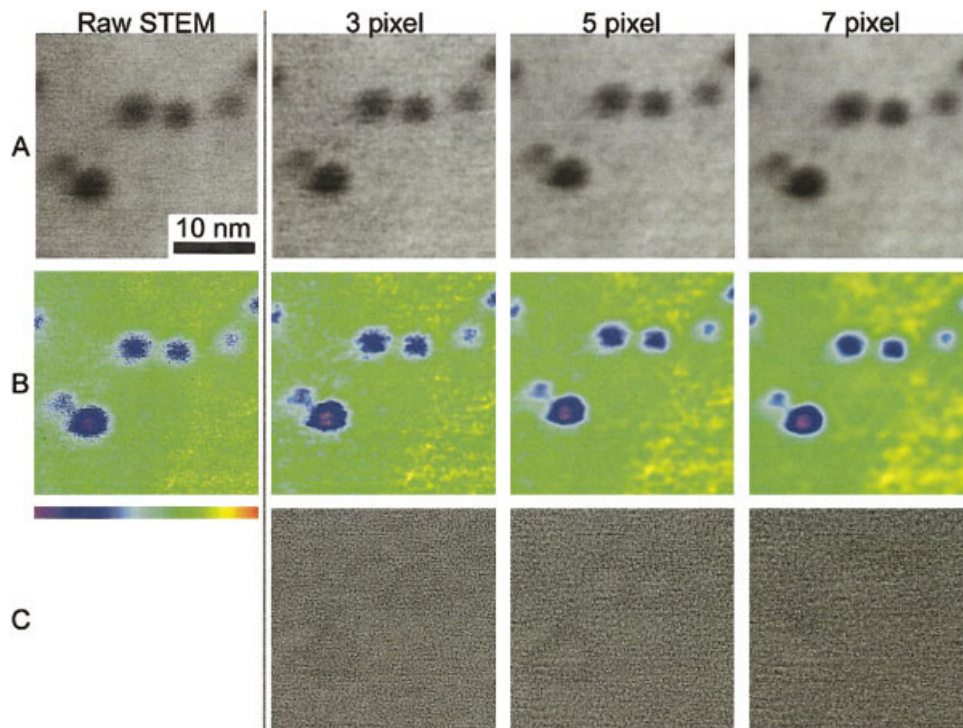


Figure 2. Comparison of a raw STEM image versus image models created with different sized point-response functions with an Airy disc shape. The PRF pixel size for the image models is indicated at the top of each column. Row A contains grayscale images, row B contains false colored images, and row C contains the residuals. The material is a fully neutralized Zn-SMAA.

tion (PRF), in this case a simulated probe of a given size and shape. The result is called the image model. To check the quality of the deconvolution, the image model is convolved with PRF to produce a noise-free image called the data model. The differences between a raw STEM image and a data model are called the residuals and provide a point-by-point measure of the noise that arises from the electron optics. Residuals that look like random noise with no apparent spatial structure and an appropriate frequency distribution indicate that the original data were of high quality and that the deconvolution was successful.

The images in this article were acquired with a 0.7-nm full width at half-maximum (FWHM) electron probe with an Airy disc shape [Fig. 1(a)]. Because attempts to directly image the electron probe were unsuccessful, a simulated PRF was used. The size and shape of PRF were examined to determine how they impact the image model. The expectation is that the simulated conditions that best represent the real STEM electron probe will be the most appropriate for the deconvolutions.

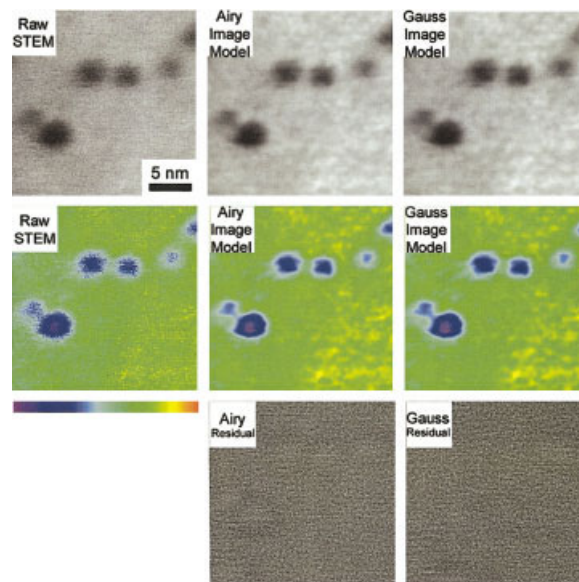


Figure 3. Comparison of a raw STEM image versus image models created with different shaped point-response functions with a 0.7-nm-diameter PRF. The PRF shape is indicated in each image. The top row contains grayscale images, the middle row contains false-colored images, and the bottom row contains the residuals. The material is a fully neutralized Zn-SMAA.

A raw STEM image of Zn-SMAA was deconvolved with a simulated PRF with 3, 5, and 7 pixel fwhms. Each pixel of this raw STEM image corresponds to 0.14 nm; therefore, the simulated PRF sizes were 0.42, 0.70, and 0.98 nm, respectively. The resulting image models were examined in both grayscale and false color, and the featureless residuals indicate a high-quality and reliable deconvolution (Fig. 2). The grayscale raw STEM image reveals an ionomer morphology consisting of solid spherical ion-rich aggregates in an ion-poor matrix (see refs. ¹⁻⁴ for details of the image interpretation). Upon false coloring of this image, the aggregates appear in blue and purple, whereas the ion-poor regions are green or yellow. Much of the detail in the raw STEM image is obscured because of the high noise level.

Selection of the correct PRF width is of great importance for proper image reconstruction. If the PRF is too broad, real details in the image will be lost. If the PRF is too narrow, the resolution gain will be less than optimal. Consequently, all of the subsequent deconvolutions were performed with the appropriate simulated PRF with a fwhm of 5 pixels, or 0.70 nm, corresponding to the fwhm used during STEM imaging. In addition, use of the Pixon method ensures that random, stochastic noise is strongly suppressed in the image models because all features must pass stringent statistical tests. The user selects the stringency of these tests on the basis of the nature of the data and the imaging goals, for example, weaker real features can be included in the image model at the risk of passing a larger number of false features. The reconstructions performed in this article were rather conservative to ensure that any features present in the image model have a very low probability of being produced by stochastic noise. Any structures that appear in the image models are highly reliable and result from real structures in the raw STEM image or unknown and unmodeled systematic effects in the microscope.

The same raw STEM image as before was also deconvolved with a 5-pixel simulated PRF with a shape of a Gaussian and an Airy disc (Fig. 3). Again, both grayscale and false color were used to compare the image models with the raw STEM image. As expected, Pixon processing of both simulated PRFs result in a decrease in the noise level of the image models as compared with the raw STEM image. There is a noticeable difference between the two image models due to the simulated PRF shape, with the features in the Airy-decon-

volved reconstruction being smaller on average than those in the Gaussian-deconvolved reconstruction. This is because the contributions to the image from the outer maxima of an Airy function are significantly larger than those of a Gaussian function. Therefore, in the Airy deconvolution the contributions of nearby structures are more correctly removed, allowing features to show their true size. We conclude that the deconvolved STEM images or image models best represent the true morphology when using an Airy-shaped PRF profile. As such, all subsequent deconvolutions were performed with the appropriate simulated PRF shape of an Airy disc. In addition, all subsequent raw STEM images are presented in grayscale, and all image models are portrayed in false color.

RESULTS AND DISCUSSION

A raw STEM image of Zn-SMAA was investigated to determine the impact of deconvolution beyond the noise-level reduction previously described. The aggregates in Zn-SMAA are spherical in shape, randomly distributed throughout the section, and approximately 4 nm in diameter (Fig. 4). In the raw STEM image, the edges of the aggregates are difficult to discern, which makes precisely measuring the aggregate diameter a challenging task. However, in the image model, the edges of the aggregates are more easily identifiable. This makes it easier to measure the aggregate dimensions. A comparison of the average diameters and standard deviations indicates that although the measurement of the aggregates in the image model is simplified, the mean aggregate diameter does not change. Specifically, the average aggregate diameters were 4.0 ± 0.7 and 4.0 ± 0.8 nm for the raw images and image models, respectively. Therefore, it is not imperative to deconvolve raw STEM images before measuring nanometer-scale objects, although deconvolution does facilitate the process.

The deconvolution also makes it easier to distinguish if there are aggregates that are overlapped in the projected image. Consider the higher-magnification images in Figure 5(a,b). From the grayscale raw STEM image, we surmised that the L-shaped feature is most likely the overlap of multiple spherical aggregates. Upon deconvoluting, multiple maxima are observed in the L-shaped feature and the feature in the upper left corner of the image, and a single maximum is

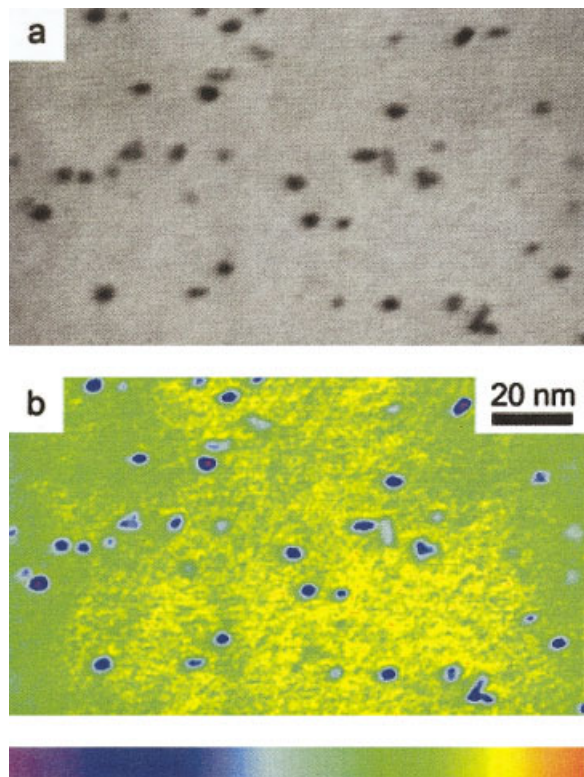


Figure 4. Lower-magnification images of the Zn-SMAA ionomer morphology: (a) grayscale raw STEM image and (b) false-colored image model.

observed in the other feature. This suggests that the L-shaped feature is a projection of four aggregates, the feature in the upper left corner is a projection of two aggregates, and the other feature is a single aggregate. The four aggregates creating the L-shaped feature are centered with one at either leg of the L and two at the elbow of the L, and the two aggregates in the upper left corner feature are centered at the locations of the two maxima [as marked by an “x” in Fig. 5(b)].

Finally, and possibly most importantly, deconvolution of the STEM images allows us to more thoroughly investigate the composition profiles across aggregates. A line scan through the center of a three-dimensional solid sphere with a sharp interface [Fig. 6(a)] has a profile in the form of a step function. Features in STEM images are actually two-dimensional projections of three-dimensional objects; therefore, the intensity profile across a projection of a solid sphere is not a step function; see the solid line in Figure 6(c). However, a comparison of this intensity profile for a solid sphere with the intensity profile across an actual aggregate in a model image [Fig. 6(c), cir-

cles] indicates that the fit is poor, suggesting that the aggregates in Zn-SMAA may not be solid spheres.

Consider the same situation for a “Gaussian sphere,” that is, a radially symmetric object with a Gaussian radial density profile. A line scan

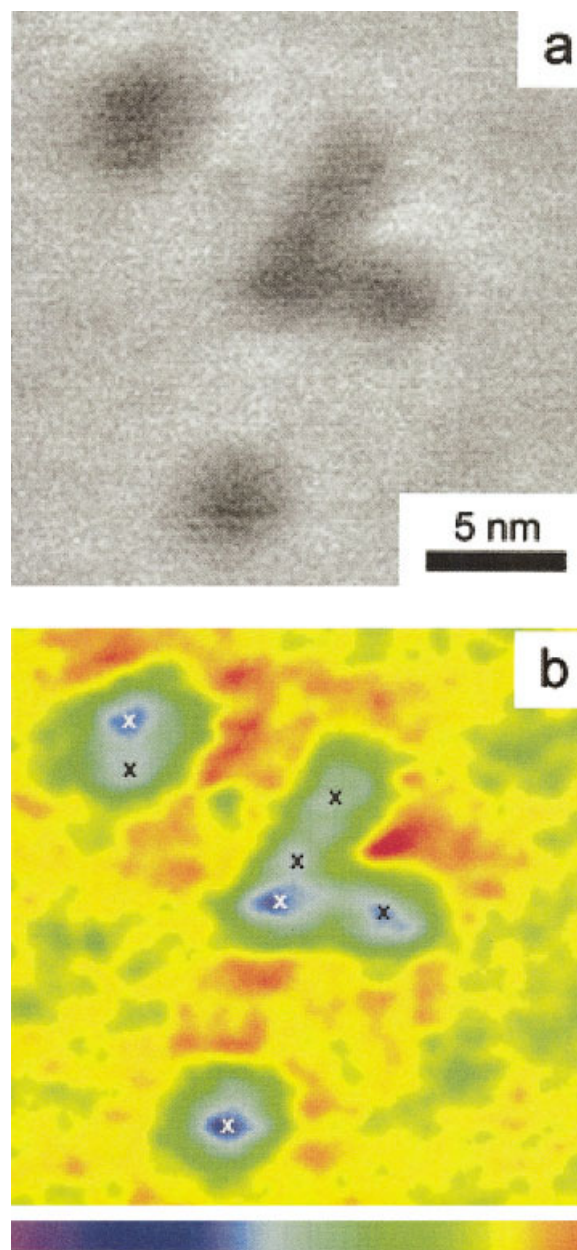


Figure 5. High-magnification images of the Zn-SMAA ionomer morphology: (a) grayscale raw STEM image and (b) false-colored image model. The images show both the decrease in the noise level and the multiple brightness maxima in various ionic aggregates, indicating an overlap of ionic aggregates in the projection. Each “x” indicates a brightness maximum.

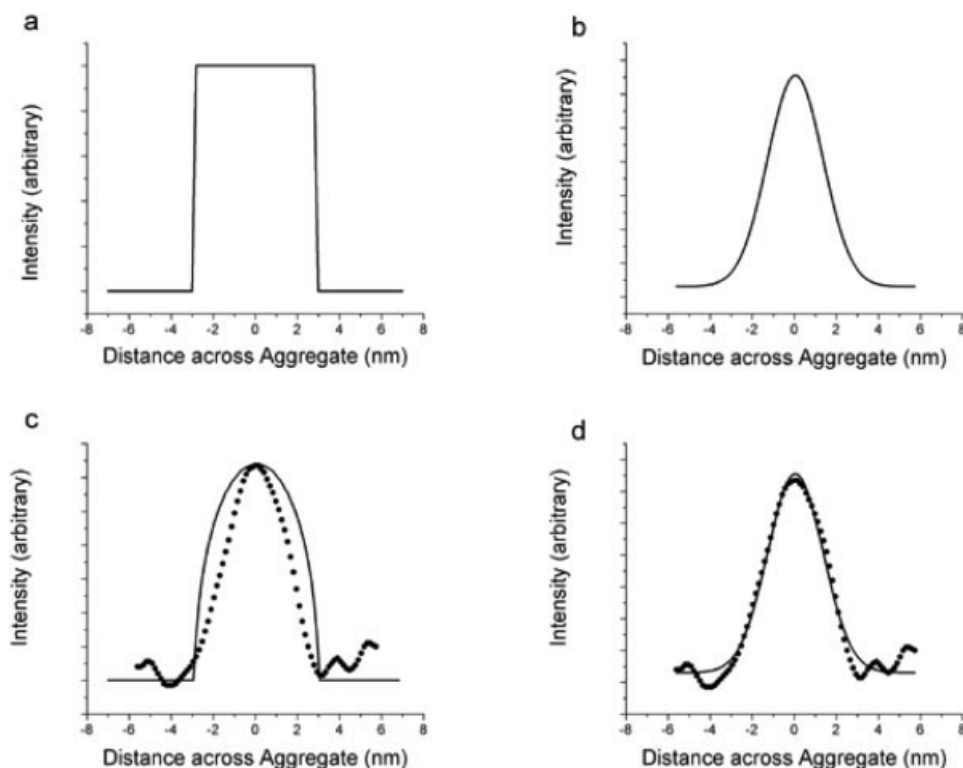


Figure 6. (a) Line scan through the center of a three-dimensional solid sphere, (b) line scan through the center of a three-dimensional Gaussian sphere, (c) intensity profile across a projected ionic aggregate in Zn-SMAA (●) and the best-fit curve of the intensity profile across a projected three-dimensional solid sphere (—), and (d) intensity profile across a projected ionic aggregate in Zn-SMAA (●) and the best-fit curve of the intensity profile across a projected three-dimensional Gaussian sphere (—).

through the center of a three-dimensional Gaussian sphere is given in Figure 6(b). The intensity profile across a projection of a Gaussian sphere is given in Figure 6(d) (solid line). A comparison of this intensity profile with that of an aggregate in an image model [Fig. 6(d), circles] indicates an excellent fit, suggesting that the aggregates in Zn-SMAA are more likely to be Gaussian spheres than solid spheres. The best fit for this aggregate is given by the FWHM of a Gaussian sphere of 3.1 nm. This particular aggregate has a diameter of 5.7 nm in the image model. The diameter measured from the projected image is more than 80% larger than the FWHM of the Gaussian sphere.

This observation leads to an interesting assessment of a previous comparison^{3,4} of STEM data with small-angle X-ray scattering (SAXS) models. Previous STEM measurements indicate that aggregates in poly(ethylene-*ran*-methacrylic acid) ionomers (EMAA) melt-neutralized to a level of 78% with Zn are nominally 2.1-nm-diameter spheres.⁴ However, the application of the Yarusso-Cooper

model to fit SAXS data of similar Zn-EMAA ionomers results in an aggregate diameter of ~ 0.9 nm.¹⁰ The Yarusso-Cooper model assumes hard spheres and interparticle scattering; therefore, the reported diameter does not consider a compositional variation within the ionic aggregates. If the aggregates are actually Gaussian rather than solid spheres, it is possible that the Yarusso-Cooper model reports a FWHM of a Gaussian profile rather than a diameter of a solid sphere. This would result in the “diameter” as reported from SAXS as being significantly smaller than the “diameter” reported from STEM. Although this is an interesting postulation, additional research is necessary.

CONCLUSIONS

This study is an important step with STEM to quantitatively image ionomer morphologies. Deconvolution of raw STEM images of ionomers greatly decreases the noise level in the images and allows

for the more rigorous investigation of ionic aggregate morphologies. The deconvolutions of the STEM images of Zn-SMAA ionomers indicate that the raw STEM images accurately depict the ionomer morphology of these materials. The dimensions of the ionic aggregates in the raw STEM images and image models are indistinguishable on the basis of a comparison of the simulated probe conditions. However, with the assistance of deconvolution, the composition profile across the ionic aggregate appears to be a Gaussian sphere rather than a solid sphere. The overall result of this work is that deconvolution of STEM images can provide ways in which to improve our investigations of the morphologies of ionomers.

The authors thank Andreas Taubert and Doug Yates (University of Pennsylvania) for their microscopy expertise. The authors also acknowledge Joon-Seop Kim and Ju-Myoung Song (Chosun University, Korea) for providing the SMAA copolymer and Joyce Tam (University of Pennsylvania) for performing the neutralization reactions. This research was funded in part by NSF-DMR 99-06829.

REFERENCES AND NOTES

1. Kirkmeyer, B. P.; Taubert, A.; Kim, J.-S.; Winey, K. I. *Macromolecules* 2002, 35, 2648–2653.
2. Kirkmeyer, B. P.; Weiss, R. A.; Winey, K. I. *J Polym Sci Part B: Polym Phys* 2001, 39, 477–483.
3. Laurer, J. H.; Winey, K. I. *Macromolecules* 1998, 31, 9106–9108.
4. Winey, K. I.; Laurer, J. H.; Kirkmeyer, B. P. *Macromolecules* 2000, 33, 507–513.
5. Taubert, A.; Winey, K. I. *Macromolecules* 2002, 35, 7419–7426.
6. Williams, D. B.; Carter, C. E. *Transmission Electron Microscopy: A Textbook for Materials Science*; Plenum: New York, 1996.
7. Kadavanich, A. V.; Kippeny, T. C.; Erwin, M. M.; Pennycook, S. J.; Rosenthal, S. J. *J Phys Chem B* 2001, 105, 361–369.
8. Puetter, R. C.; Yahil, A. *Proceedings of Astronomical Data Analysis Software and Systems VIII*, Urbana, IL, 1998, Mehringer, D. M.; Plante, R. L.; Roberts, D. A., Eds. *Astronomical Society of the Pacific*, San Francisco, CA, pp 307–316.
9. <http://www.pixon.com/brochure.html>, Example 15.
10. Yarusso, D.; Cooper, S. L. *Polymer* 1985, 26, 371–378.